

# UniView: Enhancing Novel View Synthesis From A Single Image By Unifying Reference Features

HAOWANG CUI and RUI CHEN\*, Tianjin Key Laboratory of Imaging and Sensing Microelectronic Technology, School of Microelectronics, Tianjin University, China  
TAO LUO, School of Cyber security, Tianjin University, China  
RUI LI\*, China Electronics System Technology Co., Ltd., China  
JIAZE WANG, Tianjin Key Laboratory of Imaging and Sensing Microelectronic Technology, School of Microelectronics, Tianjin University, China

The task of synthesizing novel views from a single image is highly ill-posed due to multiple explanations for unobserved areas. Most current methods tend to generate unseen regions from ambiguity priors and interpolation near input views, which often lead to severe distortions. To address this limitation, we propose a novel model dubbed as UniView, which can leverage reference images from a similar object to provide strong prior information during view synthesis. More specifically, we construct a retrieval and augmentation system and employ a multimodal large language model (MLLM) to assist in selecting reference images that meet our requirements. Additionally, a plug-and-play adapter module with multi-level isolation layers is introduced to dynamically generate reference features for the target views. Moreover, in order to preserve the details of an original input image, we design a decoupled triple attention mechanism, which can effectively align and integrate multi-branch features into the synthesis process. Extensive experiments have demonstrated that our UniView significantly improves novel view synthesis performance and outperforms state-of-the-art methods on the challenging datasets.

CCS Concepts: • **Information systems** → **Multimedia content creation**.

Additional Key Words and Phrases: Diffusion model, Novel view synthesis, Retrieval-augmented generation, Multimodal large language model

## ACM Reference Format:

Haowang Cui, Rui Chen, Tao Luo, Rui Li, and Jiaze Wang. 2025. UniView: Enhancing Novel View Synthesis From A Single Image By Unifying Reference Features. In *Proceedings of Make sure to enter the correct conference title from your rights confirmation email (Conference acronym 'XX)*. ACM, New York, NY, USA, 17 pages. <https://doi.org/XXXXXXX.XXXXXXX>

\*Corresponding author

Authors' Contact Information: [Haowang Cui](mailto:haowangcui@tju.edu.cn), [haowangcui@tju.edu.cn](mailto:haowangcui@tju.edu.cn); Rui Chen, [ruichen@tju.edu.cn](mailto:ruichen@tju.edu.cn), Tianjin Key Laboratory of Imaging and Sensing Microelectronic Technology, School of Microelectronics, Tianjin University, Tianjin, China; Tao Luo, School of Cyber security, Tianjin University, Tianjin, China, [luo\\_tao@tju.edu.cn](mailto:luo_tao@tju.edu.cn); Rui Li, China Electronics System Technology Co., Ltd., Beijing, China, [rui.li@cestc.cn](mailto:rui.li@cestc.cn); Jiaze Wang, Tianjin Key Laboratory of Imaging and Sensing Microelectronic Technology, School of Microelectronics, Tianjin University, Tianjin, China, [jiaze\\_w@tju.edu.cn](mailto:jiaze_w@tju.edu.cn).

Permission to make digital or hard copies of all or part of this work for personal or classroom use is granted without fee provided that copies are not made or distributed for profit or commercial advantage and that copies bear this notice and the full citation on the first page. Copyrights for components of this work owned by others than the author(s) must be honored. Abstracting with credit is permitted. To copy otherwise, to republish, to post on servers or to redistribute to lists, requires prior specific permission and/or a fee. Request permissions from [permissions@acm.org](mailto:permissions@acm.org).

Conference acronym 'XX, Woodstock, NY

© 2025 Copyright held by the owner/author(s). Publication rights licensed to ACM.

ACM ISBN 1551-6865-XXXX-X/XXXX/XX

<https://doi.org/XXXXXXX.XXXXXXX>

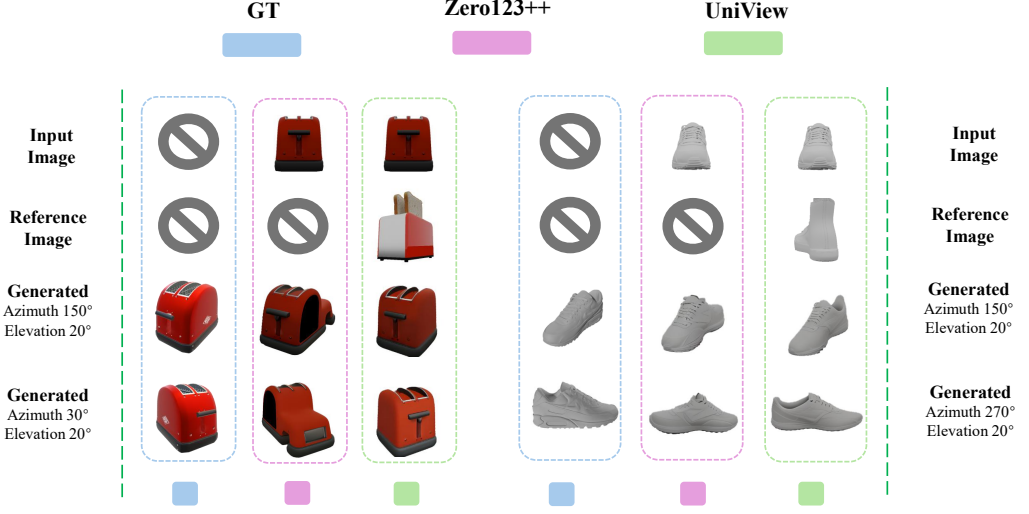


Fig. 1. Visualization results between Uniview and baseline. Compared with models that solely utilize a single image as input, our UniView can significantly enhance single-image novel view synthesis performance under challenging input viewpoints. This enhancement is achieved by incorporating complementary views from similar reference objects, particularly for regions that are entirely occluded in the original input image.

## 1 Introduction

Novel view synthesis (NVS) has long been a fundamental task in the field of 3D generation[25, 28, 46] and 3D reconstruction[10, 39, 51]. Models for novel view synthesis using multiple images of the same object from different viewpoints have achieved impressive results[20, 29]. However, this presents a challenge in terms of input data. In practice, it is often difficult for users to capture multiple images of the target object from different perspectives, especially when the input image is generated by text-to-image models[35, 36]. In such cases, synthesizing high-fidelity and high-quality novel views from a single RGB image becomes particularly crucial. Consequently, single-image novel view synthesis has emerged as a prominent area of research in computer vision.

Recent advances in generative models, particularly diffusion model-based[16, 43, 44] novel view synthesis frameworks, have been widely adopted. These models conceptualize novel view synthesis as an image-to-image generation task[3, 49], achieving both high fidelity and strong generalization capabilities. As a pioneering work, Zero123[26] generalized single-image novel view synthesis models from specific object categories to arbitrary categories, significantly enhancing their generalization capability. Specifically, Zero123++ fine-tuned a pre-trained Stable Diffusion[36] model which already containing substantial 3D priors – using 2D images rendered from 3D object data across different viewpoints. Zero123[26] posits that injecting camera transformation information into the image generation process enables effective extraction of these inherent 3D priors for novel view synthesis. Subsequent improvements[24, 27, 40] building upon Zero123[26] have enhanced both the generative quality and spatial consistency in single-image novel view synthesis.

However, synthesizing novel views of an object from a single input image, especially when the input perspective is highly challenging, is an extremely constrained and exceedingly difficult task. For regions of the object that are completely invisible in the input view, the model must rely on learned priors to hallucinate their appearance. This often results in significant distortions, such as a shoe being generated with two toe sections instead of one, as illustrated in Figure 1.

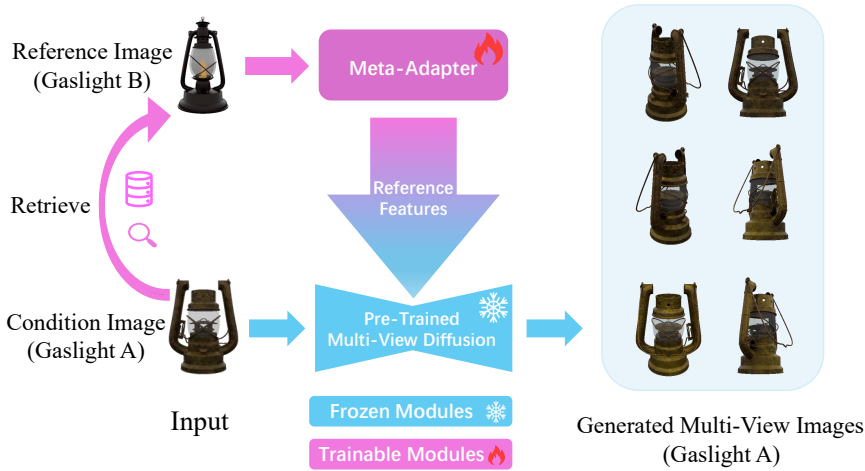


Fig. 2. The overall architecture of UniView. It retrieves the reference image from pre-constructed database and utilizes a Meta-Adapter to convert the reference image into an adaptive dynamic reference signal, which is then injected into a pre-trained multi-view diffusion model, thereby enhancing the quality of novel view synthesis.

Some works have proposed to incorporate additional control conditions into single-image novel view synthesis models in order to address the issue of poor reconstruction in invisible regions. Specifically, TOSS[41] introduced the use of a set of text prompts as control conditions to provide global information, which could enhance the quality of back-side generation in single-image novel view synthesis. However, text is inherently limited in its capacity to accurately depict object features, and relying solely on text often results in insufficiently precise control.

"Good artists copy, great artists steal." – Pablo Picasso's adage reveals an essential truth in artistic creation: faithful recreation stems from strategic appropriation. Inspired by Picasso's philosophy, we propose that: "Good models generate, great models transplant." Acquiring multi-view images of a target object has been challenging in practical scenarios, while obtaining images of arbitrary objects from the same category is relatively straightforward. For instance, when only possessing a single image of a specific shoe, we can utilize complementary viewpoint images which are from different shoes within the same category as reference for novel view synthesis. Following this principle, we present UniView - a novel framework which is capable of transferring complementary visual information from similar reference objects (e.g., the back view of shoe B) to guide novel view synthesis of target objects (e.g., shoe A). As demonstrated in Figure 1, image-based references from complementary regions of analogous objects serve as a powerful and precise control signal, significantly improving the synthesis quality of unobserved regions in the original input view.

However, the inherent misalignment dilemma between reference images and target objects makes it challenging to inject reference information into the pre-trained multi-view diffusion model meanwhile avoiding misleading guidance for novel view synthesis. In some scenarios, reference image acquisition would be a hindrance. To address these issues, as depicted in Figure 2, our method has designed a complete system which leverages a multimodal LLM to retrieve the most appropriate reference image form the pre-constructed database. Also, UniView introduces an adaptive architecture that dynamically modulates the intensity of the reference signal, which

ensures precise and effective control of reference images over the pre-trained single-image novel view synthesis model. The main contributions of this work are summarized as follows:

We design a **Dynamic Reference Retrieval System** which dynamically retrieve the most appropriate reference image from the pre-constructed database.

We propose a **Meta-Adapter Module** that generates adaptive dynamic reference signals from input reference images to enhance novel view synthesis quality for target objects, particularly for completely unobserved viewpoints in the input.

We develop a **Decoupled Triple Attention Mechanism** that introduces global control information from reference images into the model while preserving the pre-trained model's inherent novel view synthesis capability.

## 2 Related work

### 2.1 Diffusion models for 3D generation

Diffusion models[16, 43, 44] have demonstrated remarkable progress in the field of image generation. Due to their training stability and superior generation quality, they have surpassed previous generative methods[8, 12] and become the most widely adopted generative models in contemporary applications. Numerous studies have applied diffusion models to conditional generation tasks, including text-to-image[12, 36] and image-to-image synthesis models. The advancements in pre-trained models[34, 38] have facilitated large-scale high-resolution image generation based on diffusion models.

Given the remarkable success of diffusion models in 2D domains, an increasing number of recent works have sought to extend these approaches from 2D to 3D applications. Since 3D data is not as abundant as 2D data, many works have applied the rich priors of 2D pre-trained diffusion models to the 3D domain. For instance, the Score Distillation Sampling (SDS) loss[33] has been employed to distill knowledge from 2D models into 3D representations, enabling supervision for various 3D applications including generation[21, 56], editing[19, 60], and texturing[2, 5, 55]. With the gradual improvement of 3D datasets, more and more research has shifted to diffusion in 3D space. Some methods integrate diffusion models with 3D representations such as NeRF[9, 31], 3D Gaussian splatting[14, 58], and Triplane[42, 48]. By training directly on 3D data, these approaches significantly improved the quality and generation speed of 3D content.

Due to the immense potential demonstrated by diffusion models in the 3D domain, an increasing number of novel view synthesis methods based on diffusion models have emerged in recent years. Some works directly train diffusion models to generate multi-view images with 3D consistency[3, 49]. Alternative approaches fine-tuned pre-trained 2D diffusion models using 3D data for novel view synthesis[24, 26, 40], effectively harnessing the 3D-aware priors inherent in large-scale image generation models.

### 2.2 Novel view synthesis

Novel View Synthesis (NVS) refers to the process of generating new perspectives of a scene or objects from a limited set of input images. Traditional NVS methods relied heavily on geometry-based techniques, such as multi-view stereo[11, 52] and image-based modeling[22]. Such methods require multi-view images with exact camera calibration and depth data for 3D reconstruction. Their effectiveness is counterbalanced by dependencies on comprehensive inputs and meticulous calibration.

Recent advancements in NVS have been driven by deep learning, where Neural Radiance Fields (NeRF)[29] represent a pivotal breakthrough. NeRF is a deep learning technique used for generating highly realistic 3D renderings from 2D images. NeRF models represent a 3D scene as a continuous

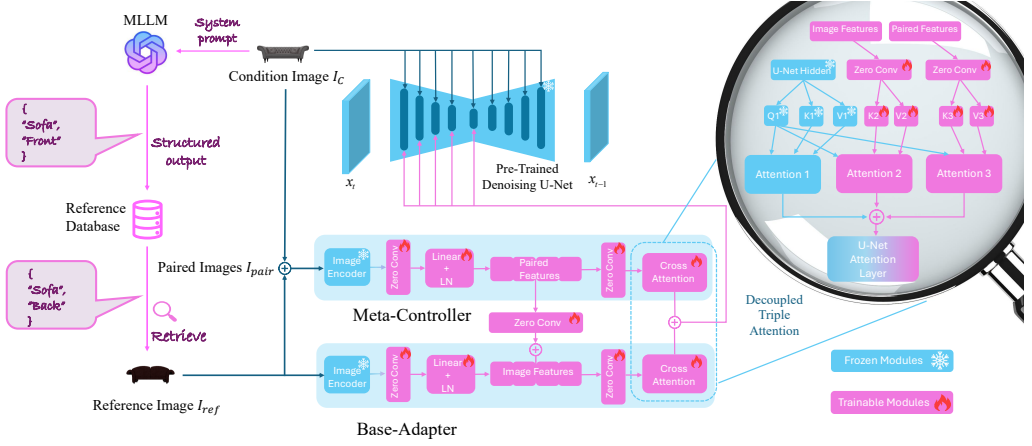


Fig. 3. The detailed architecture of UniView. The system leverages a multimodal large model to retrieve the optimal reference image from the database based on the input condition image. Then, an image pair composed of a condition image and a reference image is processed through a Meta-Adapter, which integrates a Base-Adapter and a Meta-Controller. Subsequently, the output is incorporated into a pre-trained multi-view diffusion model via a Decoupled Triple Attention mechanism. Zero convolution layers are strategically inserted between the Base-Adapter and Meta-Controller modules, as well as preceding the Decoupled Triple Attention mechanism, to ensure effective isolation.

volumetric field, allowing for the generation of images from different viewpoints by simulating light interactions. Methods based on NeRF[1, 32, 54] have shown impressive results in novel view synthesis. While NeRF has achieved high-quality novel view synthesis, it suffers from significant computational inefficiency. In recent years, 3D gaussian splatting-based approaches[17, 20, 57] have gained prominence in novel view synthesis applications. This methodology employs 3D gaussian ellipsoids to model scene representations. Novel views are synthesized by projecting these Gaussians onto the image plane via differentiable splatting. The 3D gaussian splatting framework substantially enhances rendering efficiency, thereby enabling real-time novel view synthesis capabilities.

Notwithstanding the remarkable view synthesis quality achieved by NeRF and 3D gaussian splatting approaches, these methods fundamentally require multi-view images of target objects, which poses significant challenges in data acquisition complexity. Synthesizing novel views from a single image has long been a goal pursued by researchers. The evolution of single-image novel view synthesis has progressed from end-to-end systems[50] to pre-trained generative architectures[4, 26, 40], with the latter demonstrating superior synthesis fidelity.

### 3 Methodology

Our goal is to establish a novel view synthesis framework that simultaneously accepts both a condition image and a complementary-view reference image from the same object category as input. To provide our model with appropriate reference images, we construct a **Dynamic Reference Retrieval System** (Section 3.1) which is inspired by the Retrieval-Augmented Generation (RAG)[23] technique employed in large language models. This system utilizes a multimodal large language model (MLLM) to automatically select images from the database that match the input image, serving as reference images for subsequent processing stages.

With reference image provided, we aim for this image to provide global information about the target object while avoiding interference with the control of the condition image. As a type of

image diffusion model that incorporates camera viewpoint information, multi-view diffusion models are particularly well-suited for novel view synthesis tasks. To augment a pre-trained multi-view diffusion model, we propose a reference image processing module. The features extracted by this module are adaptively fused into the frozen diffusion architecture. Our approach can utilize any multi-view diffusion model. Specifically, we employ Zero123++[40], a novel view synthesis model that takes a single condition image as input, as the base pre-trained multi-view diffusion model for our experiments.

We denote the condition image as  $I_c$  and the reference image as  $I_{ref}$ . The training objective of our diffusion model  $\epsilon_\theta$  can be then formulated as:

$$\mathcal{L} = \mathbb{E}_{t, \epsilon \sim N(0,1)} \left[ \left\| \epsilon - \epsilon_\theta(x_t, t, I_c, I_{ref}) \right\|^2 \right] \quad (1)$$

Where  $t$  is the time step,  $x_t$  is denoised feature at time  $t$  and  $\epsilon$  is the ground truth noise.

To maximize the utilization of the pre-trained prior, only the additional conditioner used for processing the reference image is trainable, while the base multi-view diffusion model remains frozen.

Two dominant approaches exist for adding image conditions to diffusion models: the Adapter[30, 53] methodology and the ControlNet[59] framework. However, directly applying these methods to our task causes over-alignment with the reference image. This severely degrades the novel view synthesis capability of the conditional generation framework. To address this challenge, we implement: **Meta-Adapter Module** (Section 3.2) with multilevel isolation for adaptive dynamic control of the conditioning strength and **Decoupled Triple Attention Mechanism** (Section 3.3) for effective feature injection. The detailed architectural of our model is illustrated in Figure 3.

### 3.1 Dynamic Reference Retrieval System

Our method allows users to manually provide a reference image  $I_{ref}$  and an condition image  $I_c$  as inputs. However, in some cases, obtaining a reference image with a complementary perspective of the same category as the condition image might be difficult. Therefore, we construct a Dynamic Reference Retrieval System to automatically select appropriate images from a database as reference images when users can not provide them.

We constructed a database comprising 20,000 images from 100 object categories. Each category contains 200 instances captured from four canonical viewpoints (front, back, left, right), with category and viewpoint annotations. As illustrated in Figure 3, when the system receives a condition image, we employ the multimodal large language model GPT-4O[18] to assist in selecting the reference image. Specifically, we predefine a system prompt that instructs the MLLM to infer the category and approximate viewpoint of the condition image, then return a structured JSON output. If the object does not belong to any of the 100 predefined categories, our system prompt guides the MLLM to provide the closest matching category label from the available 100 classes as a substitute. After receiving the MLLM's response, we parse the formatted output, first retrieving objects of the same category as the condition image, and then selecting the corresponding complementary viewpoint image as the reference image.

### 3.2 Meta-Adapter Module

The adapter module enables image control conditions for pre-trained diffusion models to achieve image-to-image translation. Processed condition images are injected into the diffusion model through the adapter to regulate its generation results. In this architecture, only the adapter remains trainable while the diffusion model remains frozen, making it a more lightweight control method for diffusion models compared with alternative control mechanisms like ControlNet[59]. However,



in our setting, the reference image is from the same category as the condition image but represents a different instance, which typically does not maintain strict alignment with the condition image. The original T2I adapter tends to strictly align the controlled generated results with the reference image, which leads to the model injecting global features of the reference image while incorporating excessive reference details, resulting in feature confusion. Therefore, the original T2I-Adapter fails to effectively handle this scenario. To this end, we propose Meta-Adapter, as shown in Figure 3, which could dynamically adjust the control strength of the reference image.

The Meta-Adapter comprises two components: a Base-Adapter and an additional Meta-Controller. The Base-Adapter, denoted as  $\mathcal{F}_{\Theta}^{base}(\cdot)$ , is composed of a frozen image encoder, trainable zero convolution layers and trainable dimension-matching layers including linear and linear normalization layers for feature dimension alignment.

The Meta-Controller, denoted as  $\mathcal{F}_{\Theta'}^{meta}(\cdot)$  shares an identical architecture with the Base-Adapter while maintaining different trainable parameters  $\Theta'$ . It takes a set of paired  $I_c$  and  $I_{ref}$  as input. After passing through the image encoder, the paired features are concatenated into a single feature before the linear and linear normalization layers. If we conceptualize the Base-Adapter as a water faucet, then the Meta-Controller serves as the valve on this faucet, dynamically controlling the intensity of reference signals. As the Meta-Controller and Base-Adapter are jointly trained, the dynamic control signals generated by the Meta-Controller are inherently adaptive. The meta control signals generated by the Meta-Controller are injected into the pre-trained diffusion model through two distinct mechanisms. On the one hand, the control signals are first processed through a zero convolution layer and subsequently combined with the output of the Base-Adapter via summation before going through the decoupled triple attention. The output of this pathway can be formally denoted as:  $y_{meta1} = \mathcal{F}_{\Theta'}^{meta}(I_{pair})$  where  $I_{pair}$  is paired  $I_c$  and  $I_{ref}$ . Then, the complete output of the Base-Adapter can be expressed as:

$$y_{base} = \mathcal{F}_{\Theta}^{base}(I_c, y_{meta1}) \quad (2)$$

On the other hand, the meta signals  $y_{meta2}$  generated by the Meta-Controller are directly injected into the pre-trained diffusion model via decoupled triple attention. Totally, the adaptive dynamic control signals  $y_{control}$  produced by the Meta-Adapter can be formulated as:

$$y_{control} = \text{CrossAttention}(y_{base}, y_{meta2}) \quad (3)$$

The Meta-Controller need not explicitly compute a matching score to control the Base-Adapter but rather learns the matching relationship implicitly in an end-to-end manner. Since the input  $I_{pair}$  of the Meta-Controller contains both the condition image and the reference image, it inherently possesses all the necessary information for comparison.

When training sample pairs  $(I_c, I_{ref})$  contain large inconsistencies, overly strong control signals  $(y_{meta1}, y_{meta2})$  from the Meta-Controller cause pathological overfitting to  $I_{ref}$ . This produces outputs that diverge from ground truth, elevating loss values. Through the backpropagation, the parameters  $\Theta'$  of the Meta-Controller would be adjusted, making it more likely to produce weaker control signals when encountering similar high-discrepancy inputs in the future. This mechanism achieves the implicit regulation.

Ultimately, when  $I_c$  and  $I_{ref}$  within the  $I_{pair}$  are highly similar, the generated  $y_{meta1}$  tends to enhance (or at least not suppress) the propagation of  $I_{ref}$  in  $\mathcal{F}_{\Theta}^{base}(\cdot)$ , allowing  $y_{base}$  to fully encode the useful geometric information from  $I_{ref}$ . Meanwhile, the generated  $y_{meta2}$  may either be zero or play a supplementary/enhancing role. Consequently, in Equation 3,  $y_{base}$  provides strong baseline guidance. The meta-control signal  $y_{meta2}$  either amplifies this strength or maintains neutrality, resulting in  $y_{control}$  dominantly reflecting reference-based conditioning.

Conversely, when  $I_c$  and  $I_{ref}$  within the  $I_{pair}$  are significantly conflicting, the generated  $y_{meta1}$  tends to suppress the propagation of conflicting features from  $I_{ref}$  in  $\mathcal{F}_{\Theta}^{base}(\cdot)$ , thereby weakening or correcting the signals in  $y_{base}$  within the conflicting regions. Simultaneously, the generated  $y_{meta2}$  will learn to produce features with opposite signs to the conflicting portions in  $y_{base}$  or generate features more aligned with  $I_c$ . Thus, in Equation 3, the signals in  $y_{base}$  are already weakened in the conflicting regions, and  $y_{meta2}$  further counteracts or overrides the adverse effects in  $y_{base}$  through additive operations. As a result, the influence from  $I_{ref}$  in  $y_{control}$  is dynamically diminished, and the control signals are predominantly governed by information consistent with  $I_c$ .

Zero convolution layer is a convolution layer with all parameters initialized to zero which can isolate newly introduced control conditions. In UniView, we introduce zero convolution layers at multiple locations. As shown in Figure 3, we position trainable zero-convolution layers at three essential locations: first after the image encoders of both Base-Adapter and Meta-Controller, second at their mutual interconnection point, and finally immediately before the decoupled cross-attention module. We denote zero convolution layers as  $\mathcal{Z}(\cdot)$ , the signal outputted by Meta-Controller before summed with Base-Adapter can be formally expressed as:

$$y'_{meta1} = \mathcal{F}_{\Theta'}^{meta}(\mathcal{Z}(I_{pair})) \quad (4)$$

and the complete output of Base-Adapter with isolation can be expressed as:

$$y'_{base} = \mathcal{F}_{\Theta}^{base}(\mathcal{Z}(I_c, y'_{meta1})) \quad (5)$$

Totally, with multilevel isolation, the adaptive dynamic control signals  $y'_{control}$  produced by the Meta-Adapter can be formulated as:

$$y'_{control} = \text{CrossAttention}(\mathcal{Z}(y'_{base}, y'_{meta2})) \quad (6)$$

These zero convolution layers ensures that during the initial training phase, the parameters of the Meta-Controller exert no influence on the Base-Adapter, while the entire Meta-Adapter's parameters also remain neutral to the original pre-trained diffusion model. The mechanism shields the diffusion backbone from initialization-induced interference, preserving the base model integrity.

### 3.3 Decoupled Triple Attention Mechanism

Our proposed method introduces a novel decoupled triple attention mechanism to effectively integrate reference information and control signals into a pre-trained multi-view diffusion model. This tripartite paradigm processes three distinct inputs through parallel cross-attention pathways: reference information, control signals, and original image features. By summing the outputs of these pathways, our model achieves a fine-grained injection of external conditions, enabling it to generate high-quality, multi-view outputs that are both consistent with the reference and guided by precise control signals.

In a U-Net[37], the down blocks progressively reduce the spatial resolution, so they capture coarse, high-level features and global structure rather than fine details. As spatial details are already compressed at this stage, injecting control signals into these early layers primarily influences the global characteristics of the generated image. In previous works on controllable image generation, such as ControlNet[59] and T2I-Adapter[30], the approach of injecting image control conditions into the down blocks was adopted. The objective of UniView is to incorporate reference image control conditions into the multi-view diffusion model while preserving the novel view synthesis accuracy of the pre-trained model. This design implies that signals from the reference image should primarily exert global control, rather than detailed control, over the generated views. Therefore, inspired by these works, UniView similarly chooses to inject control signals generated by the Meta-Adapter into the four down blocks and middle block of the diffusion model's U-Net.



For the down blocks and the middle block in base diffusion model, given the hidden feature  $f_{base}$  before attention computation, the attention feature  $Z$  can be defined by the following equation:

$$Z = \text{Attention}(Q, K, V) = \text{Softmax}\left(\frac{QK^T}{\sqrt{d}}\right)V \quad (7)$$

where  $Q = f_{base}W_q$ ,  $K = f_{base}W_k$ ,  $V = f_{base}W_v$  are the query, key, and values matrices of the attention operation.  $W_q$ ,  $W_k$ ,  $W_v$  are the weight matrices of the linear projection layers.  $f_{base}$ ,  $W_q$ ,  $W_k$  and  $W_v$  are from the U-Net of base multi-view diffusion model and are all frozen.

Given the output hidden feature from the Base-Adapter  $y_{base}$ , cross-attention  $Z'$  can be computed as:

$$Z' = \text{Attention}(Q, K', V') = \text{Softmax}\left(\frac{QK'^T}{\sqrt{d}}\right)V' \quad (8)$$

where  $Q = f_{base}W_q$ ,  $K' = y_{base}W'_k$ ,  $V' = y_{base}W'_v$  are the key, and values matrices from the Base-Adapter,  $W'_k$  and  $W'_v$  are the corresponding weight matrices.  $W'_k$  and  $W'_v$  are trainable.

Given the output hidden feature from the Meta-Controller  $y_{meta2}$ ,  $Z''$  can be computed as:

$$Z'' = \text{Attention}(Q, K'', V'') = \text{Softmax}\left(\frac{QK''^T}{\sqrt{d}}\right)V'' \quad (9)$$

where  $Q = f_{base}W_q$ ,  $K'' = y_{meta2}W''_k$ ,  $V'' = y_{meta2}W''_v$  are the key, and values matrices from the Meta-Controller,  $W''_k$  and  $W''_v$  are the corresponding weight matrices.  $W''_k$  and  $W''_v$  are trainable.

Then, we add three attention computation results together and get the the final formulation of the decoupled triple attention:

$$Z^{final} = Z + Z' + Z'' \quad (10)$$

where  $Z^{final}$  is the final attention layer we send back to the U-Net of multi-view diffusion model and replace the original attention layer  $Z$ .

Through the decoupled triple attention mechanism,  $y_{meta1}$  is fed into the Base-Adapter along with the features of  $I_{ref}$  at an earlier stage, where they jointly compute the attention matrix  $Z'$ . This allows  $y_{meta1}$  to selectively amplify or suppress feature values at different locations in  $I_{ref}$  within the Base-Adapter. Consequently, it can influence the degree to which the Base-Adapter is controlled by  $I_{ref}$  in the early stages.

Additionally, the cross-attention matrix  $Z''$  of  $y_{meta2}$  is directly added to the cross-attention matrix  $Z'$  of  $y_{base}$  via a residual connection. This enables  $y_{meta2}$  to provide a direct correction signal that facilitates more effective adjustments to  $y_{base}$ . If  $y_{base}$  contains detrimental information,  $y_{meta2}$  can learn to counteract it. If  $y_{base}$  lacks useful information,  $y_{meta2}$  can learn to supplement it. This constitutes an adjustment to the foundational control signal established by  $I_{ref}$ .

The decoupled triple attention mechanism uses a three-branch parallel architecture. This enables  $y_{meta1}$  to perform fine-grained gating during early feature extraction, while  $y_{meta2}$  facilitates direct, broad-scope adjustments at the final stage. Also, When the model injects features through cross-attention rather than direct addition, it learns higher-level abstract features and avoids negative interference from  $I_{ref}$ .

## 4 Experiments

In this section, we present the experimental deployment and results of UniView. In Section 4.1, we provide detailed descriptions of the dataset preparation. In section 4.2, we introduce how we construct our database for the retrieval system. In Section 4.3, we introduce the quantitative and qualitative results of UniView on single-image novel view synthesis. In Section 4.4, we present ablation studies. We employ Zero123++V1.2[40] as the base pre-trained model for our experiments, using clip-vit-large-patch14[34] as the image encoder and set inference steps to 75.

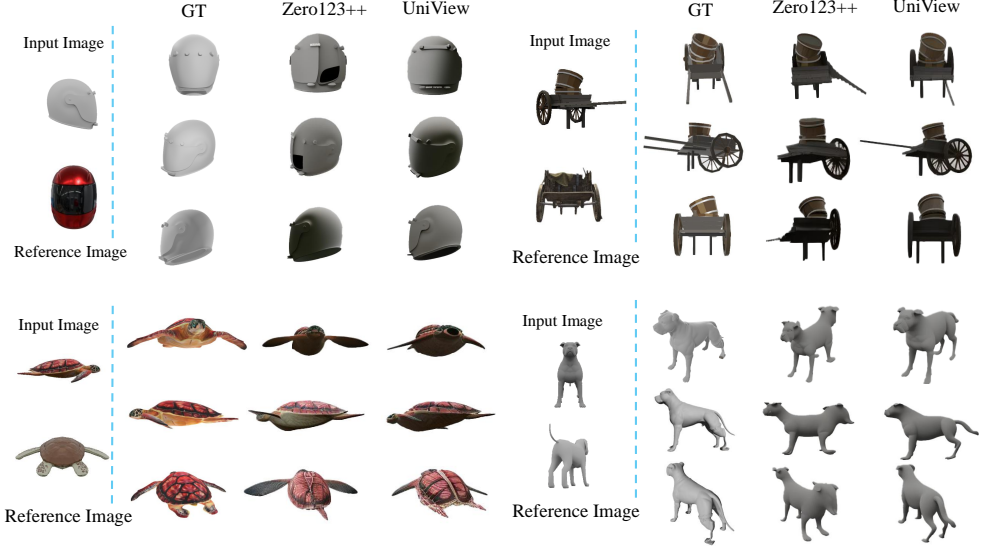


Fig. 4. Qualitative results of UniView and the baseline.

#### 4.1 Dataset preparation

Objaverse[7] is a large dataset which contains over 800K 3D models with descriptive captions, tags, and animations. The Objaverse-LVIS subset comprises 46,000 3D objects spanning 1,156 categories, with all models annotated with LVIS (Large Vocabulary Instance Segmentation)[13] labels indicating their respective categories. We employ the Objaverse-LVIS subset to construct our dataset. Utilizing the LVIS labels, we sampled 20K groups of 3D objects, each group containing two objects (a and b) from the same category.

For each group of objects, we sample 7 viewpoints for object A and 1 viewpoint for object B. To make the input view more challenging, we define the camera coordinates when rendering view 1 of object A as:  $x = 0$ ,  $y = -\text{camera distance} \approx -1.0$ ,  $z = 0$ , with  $\text{FOV} = 49.13^\circ$  and focal length = 49.13 mm. The azimuth angles are set to  $0^\circ$ ,  $90^\circ$ ,  $180^\circ$ , and  $270^\circ$ , with elevation angle =  $0^\circ$  (i.e., fully frontal view, fully lateral view, or fully posterior view). Following Zero123++V1.2, we define the camera coordinates for views 2-7 of object A as: relative to view 1, azimuth angles =  $[30^\circ, 90^\circ, 150^\circ, 210^\circ, 270^\circ, 330^\circ]$  and elevation angles =  $[20^\circ, -10^\circ, 20^\circ, -10^\circ, 20^\circ, -10^\circ]$ . Views 2-7 serve as ground truth for novel view synthesis. For object B, the rendering viewpoint is defined relative to object a's view 1 with randomly sampled relative viewpoints within azimuth angles  $90^\circ$ - $270^\circ$  and elevation angles  $-30^\circ$ - $30^\circ$ , while keeping other parameters unchanged. This configuration ensures that object B's viewpoint forms complementary perspectives relative to object A's view 1.

Following Zero123++V1.2, we rendered all 20K pairs of 3D objects using Blender[6] and set the background to pure white. Subsequently, we manually eliminated samples with rendering failures, noticeable distortions, or misclassifications and ultimately selected 15K sets of high-quality rendered data to constitute our training and testing dataset.

#### 4.2 RAG database construction

As described in Section 4.1, we utilize a database comprising 20,000 images as the data source for our Dynamic Reference Retrieval System. To construct this database, we sampled 5,000 3D objects from

Table 1. Quantitative comparison with baselines. With challenging input view, the novel view images synthesized by UniView demonstrate superior performance across multiple visual evaluation metric.

Method	PSNR $\uparrow$	SSIM $\uparrow$	LPIPS $\downarrow$
LGM	14.81	0.778	0.237
OpenLRM	15.05	0.802	0.198
SV3D	15.74	0.796	0.229
Zero123++	14.22	0.753	0.256
<b>UniView</b>	<b>16.99</b>	<b>0.847</b>	<b>0.162</b>

the unused portions (i.e., not allocated to training, testing, or validation sets) of the Objaverse-LVIS subset, following LVIS category labels. These objects span 100 distinct categories, with 50 instances per category. Each object was rendered in Blender from four orthogonal viewpoints, corresponding to azimuth angles of  $[0^\circ, 90^\circ, 180^\circ, 270^\circ]$  at a fixed elevation angle of  $0^\circ$ . All other camera parameters and background settings remain consistent with those specified for the dataset in Section 4.1.

### 4.3 Quantitative and qualitative results

The qualitative results of UniView are shown in Figure 4. It can be observed that under challenging viewpoint conditions of the input image, the base model (Zero123++) exhibits significant artifacts in synthesized novel views, manifesting phenomena such as helmet visors being only partially rendered or dogs appearing with two heads - clear deviations from ground truth. When introducing a reference image through our UniView framework, the generation quality demonstrates substantial improvement, with no recurrence of such artifacts.

We conducted a quantitative evaluation of UniView on the Objaverse dataset. From the filtered 15K paired data, we randomly selected 100 pairs as the test set and reported various visual evaluation metrics (PSNR, SSIM, LPIPS). Since there are currently no other methods similar to UniView that utilize reference images to enhance single-image novel view synthesis, we only compared against several open-source single-image novel view synthesis models and single-image 3D reconstruction models as baselines. We compared UniView with the following methods: LGM[45], OpenLRM[15], SV3D[47], and also our baseline model, Zero123++[40]. As shown in Table 1, compared with base model Zero123++ and other single-image novel view synthesis or single-image 3D reconstruction models, UniView incorporating reference images demonstrates superior performance across all metrics.

We also conducted experiments to investigate the impact of reference image quality on model performance. Specifically, we employed the following three types of references for testing: complementary views of same-category objects, complementary views of identical objects, and irrelevant objects. Qualitative and quantitative results are presented in Figure 5 and Table 2 respectively.

Our experiments have revealed that while higher-quality reference images yield marginal improvements in model performance, employing complementary views of same-category objects as references still achieves satisfactory novel view synthesis quality. However, a significant performance degradation occurs when irrelevant objects are used as references. We hypothesize that this stems from the training data composition—since the dataset exclusively contains paired samples from the same category, reference images completely unrelated to the input image may introduce confusion to the model.

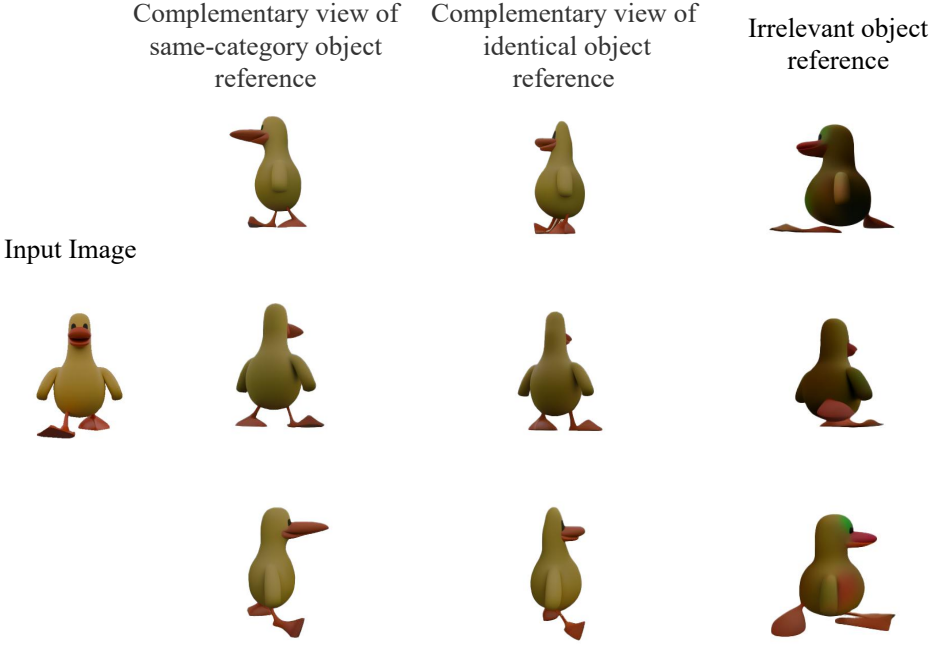


Fig. 5. Qualitative Comparison: Impact of reference image quality on model output.

Table 2. Quantitative results of the impact of reference image quality on model performance.

Reference Image	PSNR $\uparrow$	SSIM $\uparrow$	LPIPS $\downarrow$
Same-category	16.99	0.847	0.162
<b>Identical</b>	<b>17.32</b>	<b>0.855</b>	<b>0.158</b>
Irrelevant	15.76	0.661	0.243

#### 4.4 Ablation studies

To validate the correctness of our Meta-Adapter architecture, we conducted ablation studies under: Zero 123++ with Base-Adapter only, Zero 123++ with Base-Adapter and Meta-Controller, Zero 123++ with Base-Adapter, Meta-Controller and zero convolution (i.e., the complete UniView structure). The qualitative results of the ablation studies are shown in Figure 6, the quantitative results are shown in Table 3.

To validate the effectiveness of the Meta-Controller, we compared the performance of using only the Base-Adapter versus the Base-Adapter with the Meta-Controller. When using only the Base-Adapter, we removed the Meta-Controller and zero convolution structures from the complete UniView framework. The reference image was processed by the Base-Adapter without zero convolution, and the resulting image features were injected into the pre-trained Zero123++ model via dual-path decoupled cross attention. When using the Base-Adapter with Meta-Controller, we retained the Meta-Controller—which takes paired images consisting of the reference image and

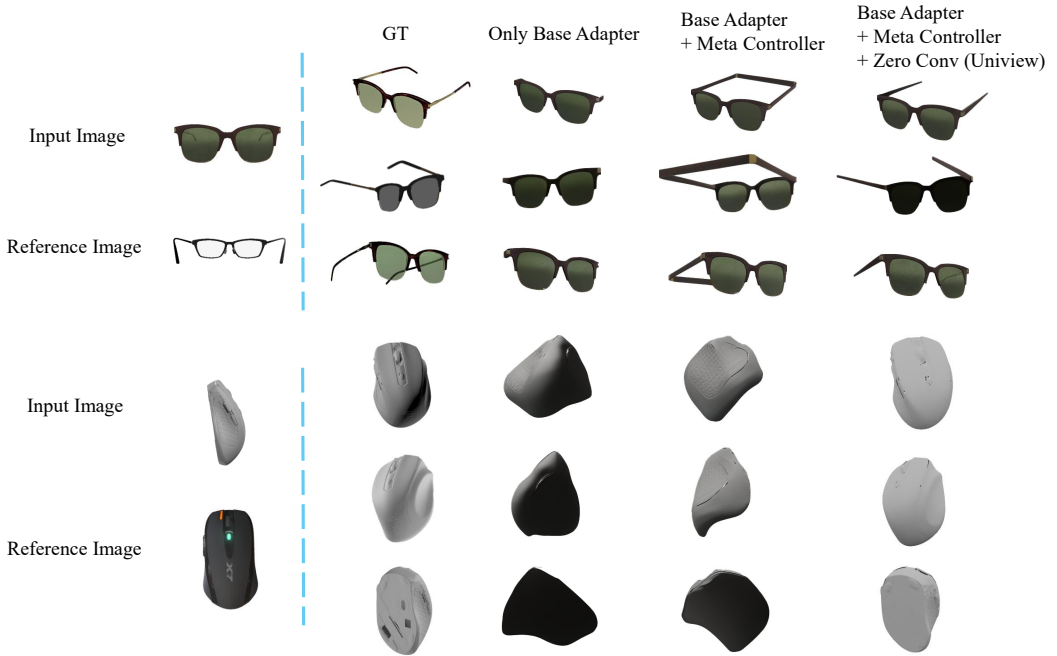


Fig. 6. Qualitative results of ablation studies.

condition image as input—while removing the zero convolution structure from the complete Uniview framework. In this setup, the paired features generated by the Meta-Controller were directly added to the image features produced by the Base-Adapter, and no zero convolution was applied to isolate the paired features and image features before their injection into the pre-trained Zero123++ model via decoupled triple attention. As illustrated in Figure 6 and Table 3, when using only the Base-Adapter, the generated results exhibited significant visual and quantitative degradation, even underperforming the original Zero123++. This indicates that directly injecting reference image features into the pre-trained model severely impairs its novel view synthesis capability. When the Meta-Controller was incorporated, the model's performance improved but still remained inferior to the complete model and even original Zero123++. This suggests that while the Meta-Controller provides a certain regulatory effect on the Base-Adapter, it still introduces adverse effects on the pre-trained model.

To validate the necessity of isolation layers, we compared the performance of Uniview with zero convolution layers removed against the complete Uniview framework. When eliminating all zero convolution layers in the model, the paired features generated by the Meta-Controller and the image features generated by the Base-Adapter were directly summed without any isolation, and these combined features were directly multiplied with the attention matrices before being injected into the pre-trained zero123++ model via decoupled triple attention mechanism. As demonstrated in Figure 6 and Table 2, the introduction of zero convolution layers significantly mitigates the degradation issue, yielding results that surpass the original zero123++. This indicates that the introduced zero convolution layers provide effective isolation, and the combined use of Meta-Controller and zero convolution is both effective and necessary.

Table 3. Quantitative results of ablation studies.

Method	PSNR $\uparrow$	SSIM $\uparrow$	LPIPS $\downarrow$
Zero123++	14.22	0.753	0.256
+ Base-Adapter	12.01	0.664	0.298
+ Meta-Controller	13.42	0.789	0.275
<b>+ Zero Conv (complete model)</b>	<b>16.99</b>	<b>0.847</b>	<b>0.162</b>

## 5 Conclusion

In this paper, we present UniView, a single-image novel view synthesis model enhanced by reference images. Through three mechanisms: the Dynamic Reference Retrieval System, Meta-Adapter and Decoupled Triple Attention, UniView automatically selects reference and effectively injects reference signals into a pre-trained multi-view diffusion model while mitigating negative interference of reference signals on the original model. UniView significantly improves the quality of single-image novel view synthesis under challenging input views, particularly for completely invisible regions in the input view. Furthermore, UniView provides an enhanced foundational component for downstream novel view synthesis-based tasks such as single-image 3D reconstruction.

## Acknowledgments

This work was supported by the National Natural Science Foundation of China under Grant 62272341.

## References

- [1] Jonathan T Barron, Ben Mildenhall, Matthew Tancik, Peter Hedman, Ricardo Martin-Brualla, and Pratul P Srinivasan. 2021. Mip-nerf: A multiscale representation for anti-aliasing neural radiance fields. In *Proceedings of the IEEE/CVF international conference on computer vision*. 5855–5864.
- [2] Tianshi Cao, Karsten Kreis, Sanja Fidler, Nicholas Sharp, and Kangxue Yin. 2023. Textfusion: Synthesizing 3d textures with text-guided image diffusion models. In *Proceedings of the IEEE/CVF International Conference on Computer Vision*. 4169–4181.
- [3] Eric R Chan, Koki Nagano, Matthew A Chan, Alexander W Bergman, Jeong Joon Park, Axel Levy, Miika Aittala, Shalini De Mello, Tero Karras, and Gordon Wetzstein. 2023. Generative novel view synthesis with 3d-aware diffusion models. In *Proceedings of the IEEE/CVF International Conference on Computer Vision*. 4217–4229.
- [4] Eric R Chan, Koki Nagano, Matthew A Chan, Alexander W Bergman, Jeong Joon Park, Axel Levy, Miika Aittala, Shalini De Mello, Tero Karras, and Gordon Wetzstein. 2023. Generative novel view synthesis with 3d-aware diffusion models. In *Proceedings of the IEEE/CVF International Conference on Computer Vision*. 4217–4229.
- [5] Dave Zhenyu Chen, Yawar Siddiqui, Hsin-Ying Lee, Sergey Tulyakov, and Matthias Nießner. 2023. Text2tex: Text-driven texture synthesis via diffusion models. In *Proceedings of the IEEE/CVF international conference on computer vision*. 18558–18568.
- [6] Blender Online Community. 2018. *Blender - a 3D modelling and rendering package*. Blender Foundation, Stichting Blender Foundation, Amsterdam. <http://www.blender.org>
- [7] Matt Deitke, Dustin Schwenk, Jordi Salvador, Luca Weihs, Oscar Michel, Eli VanderBilt, Ludwig Schmidt, Kiana Ehsani, Aniruddha Kembhavi, and Ali Farhadi. 2023. Objaverse: A universe of annotated 3d objects. In *Proceedings of the IEEE/CVF conference on computer vision and pattern recognition*. 13142–13153.
- [8] Laurent Dinh, David Krueger, and Yoshua Bengio. 2014. Nice: Non-linear independent components estimation. *arXiv preprint arXiv:1410.8516* (2014).
- [9] Ziya Erkoç, Fangchang Ma, Qi Shan, Matthias Nießner, and Angela Dai. 2023. Hyperdiffusion: Generating implicit neural fields with weight-space diffusion. In *Proceedings of the IEEE/CVF international conference on computer vision*. 14300–14310.
- [10] Yasutaka Furukawa, Carlos Hernández, et al. 2015. Multi-view stereo: A tutorial. *Foundations and trends® in Computer Graphics and Vision* 9, 1-2 (2015), 1–148.



- [11] Yasutaka Furukawa, Carlos Hernández, et al. 2015. Multi-view stereo: A tutorial. *Foundations and trends® in Computer Graphics and Vision* 9, 1-2 (2015), 1–148.
- [12] Ian Goodfellow, Jean Pouget-Abadie, Mehdi Mirza, Bing Xu, David Warde-Farley, Sherjil Ozair, Aaron Courville, and Yoshua Bengio. 2020. Generative adversarial networks. *Commun. ACM* 63, 11 (2020), 139–144.
- [13] Agrim Gupta, Piotr Dollar, and Ross Girshick. 2019. Lvis: A dataset for large vocabulary instance segmentation. In *Proceedings of the IEEE/CVF conference on computer vision and pattern recognition*. 5356–5364.
- [14] Xianglong He, Junyi Chen, Sida Peng, Di Huang, Yangguang Li, Xiaoshui Huang, Chun Yuan, Wanli Ouyang, and Tong He. 2024. Gvgen: Text-to-3d generation with volumetric representation. In *European Conference on Computer Vision*. Springer, 463–479.
- [15] Zexin He and Tengfei Wang. 2023. OpenLRM: Open-Source Large Reconstruction Models. <https://github.com/3DTopia/OpenLRM>.
- [16] Jonathan Ho, Ajay Jain, and Pieter Abbeel. 2020. Denoising diffusion probabilistic models. *Advances in neural information processing systems* 33 (2020), 6840–6851.
- [17] Binbin Huang, Zehao Yu, Anpei Chen, Andreas Geiger, and Shenghua Gao. 2024. 2d gaussian splatting for geometrically accurate radiance fields. In *ACM SIGGRAPH 2024 conference papers*. 1–11.
- [18] Aaron Hurst, Adam Lerer, Adam P Goucher, Adam Perelman, Aditya Ramesh, Aidan Clark, AJ Ostrow, Akila Welihinda, Alan Hayes, Alec Radford, et al. 2024. Gpt-4o system card. *arXiv preprint arXiv:2410.21276* (2024).
- [19] Nazmul Karim, Hasan Iqbal, Umar Khalid, Chen Chen, and Jing Hua. 2024. Free-editor: zero-shot text-driven 3D scene editing. In *European Conference on Computer Vision*. Springer, 436–453.
- [20] Bernhard Kerbl, Georgios Kopanas, Thomas Leimkühler, and George Drettakis. 2023. 3D Gaussian Splatting for Real-Time Radiance Field Rendering. *ACM Transactions on Graphics* 42, 4 (July 2023). <https://repo-sam.inria.fr/fungraph/3d-gaussian-splatting/>
- [21] Biwen Lei, Kai Yu, Mengyang Feng, Miaomiao Cui, and Xuansong Xie. 2024. DiffusionGAN3D: Boosting text-guided 3D generation and domain adaptation by combining 3D GANs and diffusion priors. In *Proceedings of the IEEE/CVF Conference on Computer Vision and Pattern Recognition*. 10487–10497.
- [22] Marc Levoy and Pat Hanrahan. 1996. Light field rendering. In *Proceedings of the 23rd Annual Conference on Computer Graphics and Interactive Techniques (SIGGRAPH '96)*. Association for Computing Machinery, New York, NY, USA, 31–42. doi:10.1145/237170.237199
- [23] Patrick Lewis, Ethan Perez, Aleksandra Piktus, Fabio Petroni, Vladimir Karpukhin, Naman Goyal, Heinrich Küttler, Mike Lewis, Wen-tau Yih, Tim Rocktäschel, et al. 2020. Retrieval-augmented generation for knowledge-intensive nlp tasks. *Advances in neural information processing systems* 33 (2020), 9459–9474.
- [24] Yukang Lin, Haonan Han, Chaoqun Gong, Zunnan Xu, Yachao Zhang, and Xiu Li. 2024. Consistent123: One Image to Highly Consistent 3D Asset Using Case-Aware Diffusion Priors. In *Proceedings of the 32nd ACM International Conference on Multimedia (Melbourne VIC, Australia) (MM '24)*. Association for Computing Machinery, New York, NY, USA, 6715–6724. doi:10.1145/3664647.3680994
- [25] Minghua Liu, Chao Xu, Haian Jin, Linghao Chen, Mukund Varma T, Zexiang Xu, and Hao Su. 2024. One-2-3-45: Any single image to 3d mesh in 45 seconds without per-shape optimization. *Advances in Neural Information Processing Systems* 36 (2024).
- [26] Ruoshi Liu, Rundi Wu, Basile Van Hoorick, Pavel Tokmakov, Sergey Zakharov, and Carl Vondrick. 2023. Zero-1-to-3: Zero-shot One Image to 3D Object. *arXiv:2303.11328* [cs.CV]
- [27] Yuan Liu, Cheng Lin, Zijiao Zeng, Xiaoxiao Long, Lingjie Liu, Taku Komura, and Wenping Wang. 2024. SyncDreamer: Generating Multiview-consistent Images from a Single-view Image. In *The Twelfth International Conference on Learning Representations*. <https://openreview.net/forum?id=MN3yH2ovHb>
- [28] Luke Melas-Kyriazi, Iro Laina, Christian Rupprecht, Natalia Neverova, Andrea Vedaldi, Oran Gafni, and Filippos Kokkinos. 2024. IM-3D: Iterative Multiview Diffusion and Reconstruction for High-Quality 3D Generation. *International Conference on Machine Learning, 2024* (2024).
- [29] Ben Mildenhall, Pratul P Srinivasan, Matthew Tancik, Jonathan T Barron, Ravi Ramamoorthi, and Ren Ng. 2021. Nerf: Representing scenes as neural radiance fields for view synthesis. *Commun. ACM* 65, 1 (2021), 99–106.
- [30] Chong Mou, Xintao Wang, Liangbin Xie, Yanze Wu, Jian Zhang, Zhongang Qi, and Ying Shan. 2024. T2i-adapter: Learning adapters to dig out more controllable ability for text-to-image diffusion models. In *Proceedings of the AAAI conference on artificial intelligence*, Vol. 38. 4296–4304.
- [31] Norman Müller, Yawar Siddiqui, Lorenzo Porzi, Samuel Rota Buló, Peter Kotschieder, and Matthias Nießner. 2023. DiffRF: Rendering-guided 3d radiance field diffusion. In *Proceedings of the IEEE/CVF Conference on Computer Vision and Pattern Recognition*. 4328–4338.
- [32] Thomas Müller, Alex Evans, Christoph Schied, and Alexander Keller. 2022. Instant Neural Graphics Primitives with a Multiresolution Hash Encoding. *ACM Trans. Graph.* 41, 4, Article 102 (July 2022), 15 pages. doi:10.1145/3528223.3530127

- [33] Ben Poole, Ajay Jain, Jonathan T. Barron, and Ben Mildenhall. 2023. DreamFusion: Text-to-3D using 2D Diffusion. In *The Eleventh International Conference on Learning Representations*. <https://openreview.net/forum?id=FjNys5c7VyY>
- [34] Alec Radford, Jong Wook Kim, Chris Hallacy, Aditya Ramesh, Gabriel Goh, Sandhini Agarwal, Girish Sastry, Amanda Askell, Pamela Mishkin, Jack Clark, et al. 2021. Learning transferable visual models from natural language supervision. In *International conference on machine learning*. PmlR, 8748–8763.
- [35] Aditya Ramesh, Mikhail Pavlov, Gabriel Goh, Scott Gray, Chelsea Voss, Alec Radford, Mark Chen, and Ilya Sutskever. 2021. Zero-shot text-to-image generation. In *International conference on machine learning*. Pmlr, 8821–8831.
- [36] Robin Rombach, Andreas Blattmann, Dominik Lorenz, Patrick Esser, and Björn Ommer. 2022. High-Resolution Image Synthesis With Latent Diffusion Models. In *Proceedings of the IEEE/CVF Conference on Computer Vision and Pattern Recognition (CVPR)*. 10684–10695.
- [37] Olaf Ronneberger, Philipp Fischer, and Thomas Brox. 2015. U-net: Convolutional networks for biomedical image segmentation. In *Medical image computing and computer-assisted intervention—MICCAI 2015: 18th international conference, Munich, Germany, October 5–9, 2015, proceedings, part III 18*. Springer, 234–241.
- [38] Chitwan Saharia, William Chan, Saurabh Saxena, Lala Li, Jay Whang, Emily L Denton, Kamyar Ghasemipour, Raphael Gontijo Lopes, Burcu Karagol Ayan, Tim Salimans, et al. 2022. Photorealistic text-to-image diffusion models with deep language understanding. *Advances in neural information processing systems* 35 (2022), 36479–36494.
- [39] Johannes L Schonberger and Jan-Michael Frahm. 2016. Structure-from-motion revisited. In *Proceedings of the IEEE conference on computer vision and pattern recognition*. 4104–4113.
- [40] Ruoxi Shi, Hansheng Chen, Zhuoyang Zhang, Minghua Liu, Chao Xu, Xinyue Wei, Linghao Chen, Chong Zeng, and Hao Su. 2023. Zero123++: a Single Image to Consistent Multi-view Diffusion Base Model. *arXiv:2310.15110* [cs.CV]
- [41] Yukai Shi, Jianan Wang, He CAO, Boshi Tang, Xianbiao Qi, Tianyu Yang, Yukun Huang, Shilong Liu, Lei Zhang, and Heung-Yeung Shum. 2024. TOSS: High-quality Text-guided Novel View Synthesis from a Single Image. In *The Twelfth International Conference on Learning Representations*. <https://openreview.net/forum?id=9ZUYJpvlyS>
- [42] J Ryan Shue, Eric Ryan Chan, Ryan Po, Zachary Ankner, Jiajun Wu, and Gordon Wetzstein. 2023. 3d neural field generation using triplane diffusion. In *Proceedings of the IEEE/CVF Conference on Computer Vision and Pattern Recognition*. 20875–20886.
- [43] Jascha Sohl-Dickstein, Eric Weiss, Niru Maheswaranathan, and Surya Ganguli. 2015. Deep unsupervised learning using nonequilibrium thermodynamics. In *International conference on machine learning*. pmlr, 2256–2265.
- [44] Yang Song, Jascha Sohl-Dickstein, Diederik P Kingma, Abhishek Kumar, Stefano Ermon, and Ben Poole. 2020. Score-based generative modeling through stochastic differential equations. *arXiv preprint arXiv:2011.13456* (2020).
- [45] Jiaxiang Tang, Zhaoxi Chen, Xiaokang Chen, Tengfei Wang, Gang Zeng, and Ziwei Liu. 2024. Lgm: Large multi-view gaussian model for high-resolution 3d content creation. In *European Conference on Computer Vision*. Springer, 1–18.
- [46] Zhenyu Tang, Junwu Zhang, Xinhua Cheng, Wangbo Yu, Chaoran Feng, Yatian Pang, Bin Lin, and Li Yuan. 2024. Cycle3D: High-quality and Consistent Image-to-3D Generation via Generation-Reconstruction Cycle. *arXiv:2407.19548* [cs.CV] <https://arxiv.org/abs/2407.19548>
- [47] Vikram Voleti, Chun-Han Yao, Mark Boss, Adam Letts, David Pankratz, Dmitry Tochilkin, Christian Laforte, Robin Rombach, and Varun Jampani. 2024. Sv3d: Novel multi-view synthesis and 3d generation from a single image using latent video diffusion. In *European Conference on Computer Vision*. Springer, 439–457.
- [48] Tengfei Wang, Bo Zhang, Ting Zhang, Shuyang Gu, Jianmin Bao, Tadas Baltrusaitis, Jingjing Shen, Dong Chen, Fang Wen, Qifeng Chen, et al. 2023. Rodin: A generative model for sculpting 3d digital avatars using diffusion. In *Proceedings of the IEEE/CVF conference on computer vision and pattern recognition*. 4563–4573.
- [49] Daniel Watson, William Chan, Ricardo Martin-Brualla, Jonathan Ho, Andrea Tagliasacchi, and Mohammad Norouzi. 2022. Novel view synthesis with diffusion models. *arXiv preprint arXiv:2210.04628* (2022).
- [50] Olivia Wiles, Georgia Gkioxari, Richard Szeliski, and Justin Johnson. 2020. Synsin: End-to-end view synthesis from a single image. In *Proceedings of the IEEE/CVF conference on computer vision and pattern recognition*. 7467–7477.
- [51] Yao Yao, Zixin Luo, Shiwei Li, Tian Fang, and Long Quan. 2018. Mvsnet: Depth inference for unstructured multi-view stereo. In *Proceedings of the European conference on computer vision (ECCV)*. 767–783.
- [52] Yao Yao, Zixin Luo, Shiwei Li, Tian Fang, and Long Quan. 2018. Mvsnet: Depth inference for unstructured multi-view stereo. In *Proceedings of the European conference on computer vision (ECCV)*. 767–783.
- [53] Hu Ye, Jun Zhang, Sibio Liu, Xiao Han, and Wei Yang. 2023. Ip-adapter: Text compatible image prompt adapter for text-to-image diffusion models. *arXiv preprint arXiv:2308.06721* (2023).
- [54] Alex Yu, Vickie Ye, Matthew Tancik, and Angjoo Kanazawa. 2021. pixelnerf: Neural radiance fields from one or few images. In *Proceedings of the IEEE/CVF conference on computer vision and pattern recognition*. 4578–4587.
- [55] Jianhui Yu, Hao Zhu, Liming Jiang, Chen Change Loy, Weidong Cai, and Wayne Wu. 2024. Painthuman: towards high-fidelity text-to-3D human texturing via denoised score distillation. In *Proceedings of the AAAI Conference on Artificial Intelligence*, Vol. 38. 6800–6807.

- [56] Xin Yu, Yuan-Chen Guo, Yangguang Li, Ding Liang, Song-Hai Zhang, and Xiaojuan Qi. 2023. Text-to-3d with classifier score distillation. *arXiv preprint arXiv:2310.19415* (2023).
- [57] Zehao Yu, Anpei Chen, Binbin Huang, Torsten Sattler, and Andreas Geiger. 2024. Mip-splatting: Alias-free 3d gaussian splatting. In *Proceedings of the IEEE/CVF conference on computer vision and pattern recognition*. 19447–19456.
- [58] Bowen Zhang, Yiji Cheng, Jiaolong Yang, Chunyu Wang, Feng Zhao, Yansong Tang, Dong Chen, and Baining Guo. 2024. GaussianCube: A Structured and Explicit Radiance Representation for 3D Generative Modeling. In *The Thirty-eighth Annual Conference on Neural Information Processing Systems*. <https://openreview.net/forum?id=DG2f1rVEM5>
- [59] Lvmin Zhang, Anyi Rao, and Maneesh Agrawala. 2023. Adding conditional control to text-to-image diffusion models. In *Proceedings of the IEEE/CVF international conference on computer vision*. 3836–3847.
- [60] Jingyu Zhuang, Chen Wang, Liang Lin, Lingjie Liu, and Guanbin Li. 2023. Dreameditor: Text-driven 3d scene editing with neural fields. In *SIGGRAPH Asia 2023 Conference Papers*. 1–10.

Received XX November 2025; revised XX XXXX XXXX; accepted XX XXXX XXXX